13th International Symposium on Particle Image Velocimetry – ISPIV 2019
Munich, Germany, July 22-24, 2019

Measurement of time response of helium-filled soap bubbles

Knud Erik Meyer*, Carl Oscar Meyer-Johansen, Ask Finderup

Technical University of Denmark, Copenhagen, Denmark

* corresponding author: kem@mek.dtu.dk

Abstract

A new method is proposed for measuring the time response of helium-filled soap bubbles (HFSB). A flow of air with bubbles is led through a square flow channel and a two dimensional slit is introduced downstream in the channel. This creates a strong local flow acceleration. Bubble paths are tracked with a camera and the time response is found by comparing bubble speed and acceleration to the local flow speed. The method can be used in a portable setup for monitoring bubble quality during experiments. Bubbles from a new bubble generator design are tested. The generator produces mono-disperse bubbles with a low time response, but data also suggest that the generator needs further optimization. Air-filled soap bubbles (AFSB) are also tested and appear to have a smaller time response than earlier reports on AFSB.

1 Introduction

There has recently been several reports on the use of helium-filled soap bubbles (HFSB) to measure air velocities in large volumes. Bosbach et al. (2009) introduced a special nozzle to generate HFSB to be used for large-scale Particle Image Velocimetry (PIV) measurements in air. Newer and more compact designs have been developed by Faleiros et al. (2019) and by Gibeau and Ghaemi (2018). Faleiros et al. (2018) have shown that Particle Tracking Velocimetry (PTV) on HFSB can give high quality measurements in a turbulent boundary layer. Volumetric large scale measurements have been demonstrated, e.g., in a thermal plume (Huhn et al., 2017) and around a full-scale cyclist (Jux et al., 2018). The time response of the bubbles is an essential property. The time response should be small for the bubbles to faithfully track the flow. Scarano et al. (2015) used the flow stagnation in front of a cylinder in a wind tunnel to measure the time response. This method was also used by Gibeau and Ghaemi (2018) and by Faleiros et al. (2019), who showed how the flow rates of helium, bubble fluid solution and air, respectively, must be controlled accurately to produce bubbles with a low time response and a uniform size distribution.

Using the stagnation flow in front of a cylinder to estimate the time response is convenient for applications in wind tunnels, but it is less convenient for measurements in other applications. The present work aims to develop an alternative and more compact method for measuring the time response of HFSB using a flow channel with a two-dimensional slit inserted at a cross section, see figure 1. This is both relevant for developing generators of HFSB and for monitoring production of bubbles at experimental setups.

2 Time response

A particle (or bubble) moving in a fluid at low particle Reynolds number can with certain approximations (here also neglecting gravity forces) be reasonably described, see Adrian and Westerweel (2011), using the equation

$$\frac{d\mathbf{v}_p}{dt} \cong \frac{\mathbf{v}_f - \mathbf{v}_p}{\tau_p} \tag{1}$$

where $\mathbf{v}_p$ is the particle velocity, $\mathbf{v}_f$ is the local fluid velocity and τ_p is the particle time constant given as

$$\tau_p = \frac{(\rho_p - \rho_f) d_p^2}{18 \rho_f \nu_f \phi} \tag{2}$$

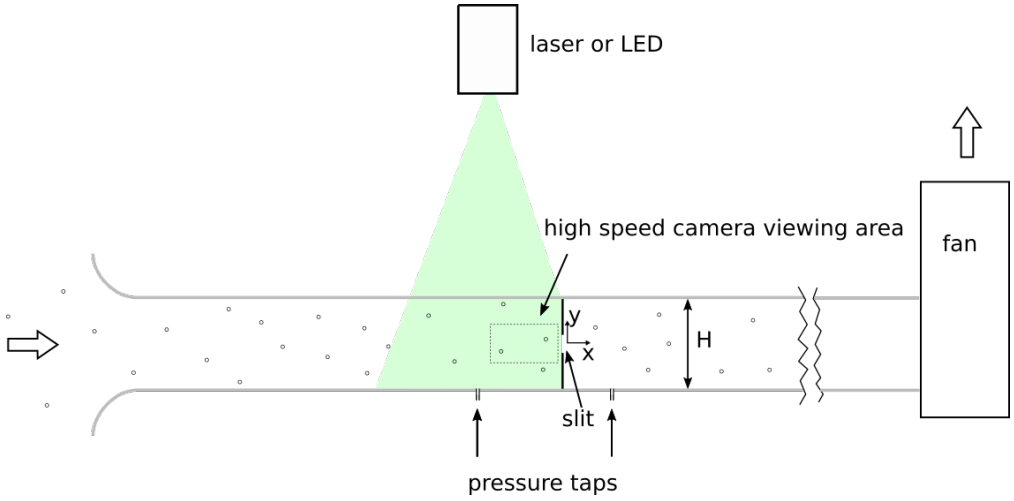

Figure 1: Sketch of the setup for measurement of bubble time response.

Here ρ_p is the average density of the particle, ρ_f is the fluid density, d_p is the particle diameter, ν_f is the kinematic viscosity of the fluid and ϕ is a term correcting the Stokes drag on the particles for the effect of moderate particle Reynolds numbers. We will refer to τ_p as the time response since it characterizes the response to a step change in fluid velocity. Note that the τ_p will take negative values if the density of the particle is lower than the density of the fluid.

From equation (1), τ_p can be estimated as

$$\tau_p = \frac{|\mathbf{v}_f - \mathbf{v}_p|}{|d\mathbf{v}_p/dt|} \tag{3}$$

The fluid velocity $\mathbf{v}_f$ is found from a separate measurement of the mean velocity field. In practice, there will be small deviations between the direction of the fluid velocity and the direction of the particle velocity, e.g. due to turbulence. To handle this, the velocities and acceleration are projected onto the direction of a local streamline of the mean flow field, i.e. in the direction of $\mathbf{v}_f$. In this way, the vectors in equation (3) can be replaced with scalar values and evaluating vector length is no longer needed. This means that τ_p can be evaluated to take negative values when $\rho_p < \rho_f$.

In previous works, e.g. Faleiros et al. (2019), the particle acceleration $d\mathbf{v}_p/dt$ has been estimated by using a polynomial fit to the particle path and evaluating $\mathbf{v}_p(d\mathbf{v}_p/dx)$ using a coordinate system where x follows the particle path. This is valid since the velocity field can be assumed to be stationary. This procedure is likely to improve the accuracy of the result since noise related to individual particle positions is averaged out. The present paper uses a different approach. The particle velocity and acceleration are evaluated using the central difference scheme on three consecutive particle positions. This can be evaluated at each particle position along a track. It is therefore possible to check that stable values are observed and to calculate the mean value for a track (a specific bubble) to get a more accurate value.

3 Experimental setup

The flow system is shown in figure 1. Air is sucked into a flow channel with a square cross section with inner side length $H = 50$ mm. The inlet to the channel has rounded edges with radius of curvature of 25 mm. A slit with a width of 10 mm is introduced in a cross section in the channel at a distance of $5H$ from the inlet. The slit is made of 0.5 mm thick steel plate and is locked in position. The flow has a strong acceleration just upstream of the slit. This is measured with a camera and a suitable light source. The coordinate system has origin in the center of the slit. The slit creates a two-dimensional flow near the mid-plane of the channel. The channel is made of transparent acrylic (PMMA) except for the side facing the camera. This side is made of glass of good optical quality. The flow is driven by a small centrifugal fan placed $7H$ downstream of the slit. Two pressure taps are located at the side wall at the mid-plane of the channel (see figure 1) with

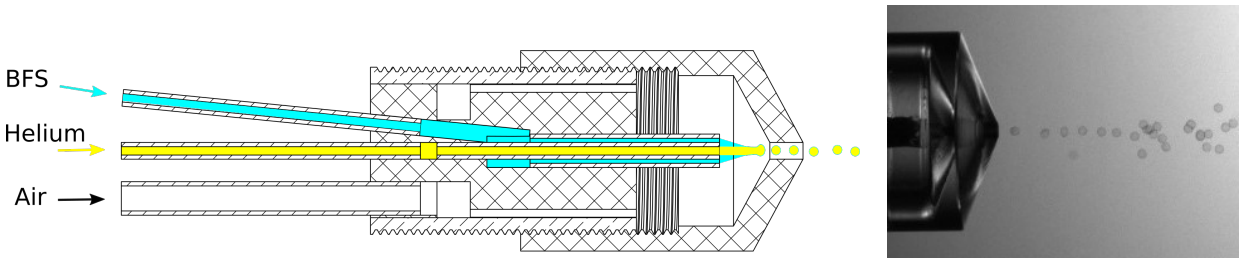

(a) Cross section (b) Visualisation

Figure 2: A cross section of the bubble generator and a visualisation of the generator in bubbling mode

one pressure tap placed $1H$ upstream of the slit and the other pressure tap placed $0.5H$ downstream of the slit. This is similar to a classic orifice plate flow meter (White, 2016). The measured pressure difference is therefore expected to be a reliable way of monitoring the flow rate in the channel. The pressure difference is measured with a Furness Controls FCO560 manometer.

The soap bubbles are produced with a generator developed at the Technical University of Denmark, see figure 2(a). The design is similar to the designs used by Faleiros et al. (2019) and Gibeau and Ghaemi (2018). The exit hole for the bubbles has a diameter of 1 mm. The inner diameter of the pipe supplying helium is 0.6 mm and the outer diameter is 1.0 mm. The inner diameter of the pipe supplying bubble fluid solution (BFS) is 1.5 mm. The air supply to the bubble formation region comes through 12 thin channels (0.5 mm height, 1.5 mm width) to provide a near uniform flow near the inside perimeter of the cap. The cap has an inner diameter of 9 mm. The cap is mounted on the rest of the nozzle with a thread and the distance between exit of helium and BFS pipes to the exit hole in the cap can therefore be adjusted. The current experiments use a distance of 4 mm.

The flow of helium to the bubble generator comes from a canister of compressed helium and the air comes from the laboratory compressed air supply. For both flows, the pressure is regulated down to a suitable working pressure and the flow is then adjusted with valves. The flow rate, for both flows, is measured with mass flow sensors from Integrated Device Technology (IDT FS2012-1020-NG). The bubble fluid solution is the SAI 1035 from Sage Action Inc. The BFS flow is driven by a syringe pump from World Precision Instruments (Aladdin 4000). The production of bubbles has been observed with shadow visualisation using light from an LED light source passing through a diffuser screen and a high speed camera (Photron Nova S9). An example is shown in figure 2(b). During the experiment the bubbles are guided towards the inlet to channel in figure 1 through a pipe with diameter of 200 mm and a length of 500 mm. The pipe is connected to the channel with a cardboard piece creating a vertical wall with an opening matching the rounded inlet edges. The bubble generator is placed 100 mm upstream of the pipe.

The mean velocity field in the channel is measured with a conventional PIV system from Dantec Dynamics using a Hisense II camera (1344 by 1024 pixels) covering the full height of the channel. The illumination comes from a Litron YAG laser with 200 mJ pulses and optics forming a light sheet with a thickness of 1 mm. The measurements use DEHS particles from a Laskin type generator. The particle diameter is about 1 μm and the particles are assumed to track the flow accurately. A calibration target with a dotted pattern and with a tight fit to the channel is used to ensure a common coordinate system with later measurements of bubbles. Images are processed to velocities using DynamicStudio ver. 6.0.

The bubble tracks are recorded with a Photron Nova S9 camera set to take 896 by 512 images at 20000 frames per second. The bubbles are illuminated from the side of the channel with a strong LED light source and a slit at the side wall limits the light to a 5 mm light sheet in the channel. The bubble tracks are found with a custom build Python code that detects positions of the two glare points from each bubble. The accurate positions of the glare points are found by cross correlation of an artificial particle image with Gaussian light distribution and a width of 3 pixels using a conventional PIV algorithm. The bubble diameter d_b is estimated in the same way as Faleiros et al. (2019) from the distance between the two glare points d_G as

$$d_b = \sqrt{2} d_G \tag{4}$$

When running the setup, a few bubbles are impacting the plates forming the slit and the walls downstream of the slit, where a quite turbulent flow is formed. However, the glass window for the camera and the side wall upstream of the slit remain clean except for a region close to the corner formed by the slit plates and the side wall. This contamination is not in the area viewed by the camera for time response evaluation

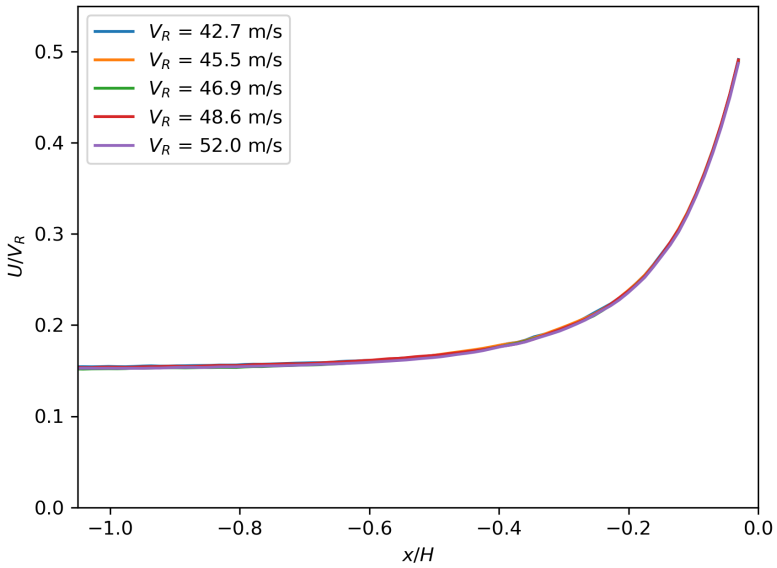

Figure 3: The U velocity component at $y = 0$ measured upstream of the slit at different flow rates.

and it does not appear to influence the light sheet going through the side wall.

4 Results

The flow field in the channel just upstream of the slit is measured at 5 different flow rates. A reference velocity V_R is defined as

$$V_R = \sqrt{\frac{2\Delta p}{\rho_f}} \tag{5}$$

where Δp is the pressure difference measured on the two pressure taps indicated in figure 1. V_R corresponds to the velocity in the *vena contracta* found slightly downstream of the slit. The velocities upstream of the slit are smaller. The velocity for $x/H < -1$ is found to be quite uniform with a velocity of $U \cong 0.15V_R$. A strong acceleration is seen for $x/H > -0.2$. The measurements at different flow rates (different Δp) are seen to collapse into one curve when normalized with V_R. This indicates that the flow here can be considered a potential flow and the effect of viscosity, mainly on the thickness of boundary layers, is negligible. The flow acceleration in the region used for estimates of time response is in the order of 10000 m/s^2.

The high speed camera observes the flow in a region of 40 mm by 23 mm just upstream of the slit, see figure 1. In this region, bubbles are tracked. As discussed in section 2, the time response is evaluated at each observed bubble position using the neighboring positions in time to estimate velocity and acceleration. However, at some distance from the slit, the flow acceleration is too small to give an accurate estimate of the time response. This is illustrated in figure 4, where a large variation in the estimated time response is seen for $x/H < -0.2$. The time response is seen to converge towards a much more narrow band of values for larger x. When following a single bubble for $x/H > -0.2$, most tracks are found to have only a small variation of the estimated time response, with standard deviation of the estimated time response in the order of 10 μs. To get reliable estimates, only values in the region with $-0.18 < x/H < -0.05$ and $-0.1 < y/H < 0.1$ are used. Furthermore, only tracks with a standard deviation of the estimated time response along the track of less than 25 μs are accepted. The accepted tracks are shown as red lines in figure 4. The mean value of the time response along a track of a bubble is used as the estimate for further analysis.

An example of the distribution of bubble diameter and time response of air-filled bubbles (AFSB) is shown in figure 5. The internal flow to the bubbles illustrated with helium in figure 2(a) is here replaced with air. The external flow of air is 57.5 l/h, the internal flow of air is 5.2 l/h and the flow of BFS is 8.9 ml/h.

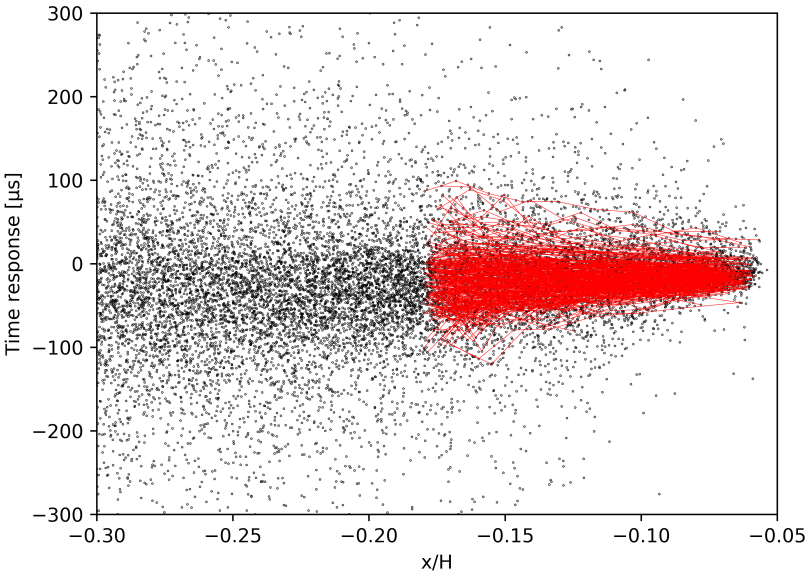

Figure 4: Example of the time response found for bubble tracks as a function of the x-position. Black dots show estimates from all bubble positions observed, red lines show tracks accepted for further analysis.

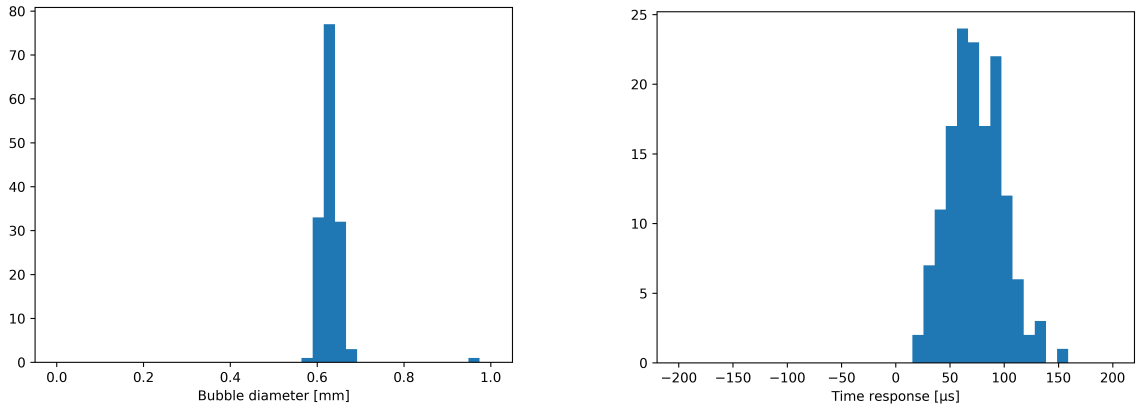

Figure 5: Example of distributions of bubble diameter and time response for air-filled soap bubbles

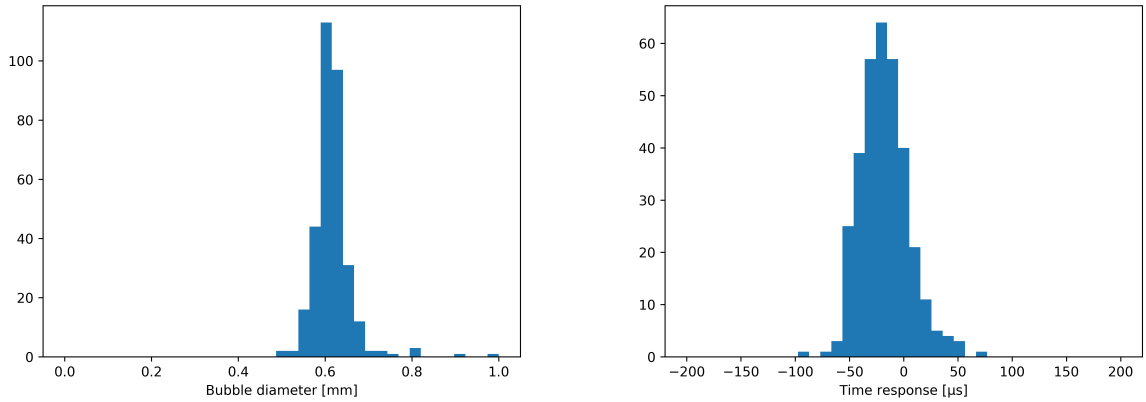

Figure 6: Example of distributions of bubble diameter and time response for helium-filled soap bubbles

An example of HFSB is shown in figure 6. Here, the external flow of air is 60.0 l/h, the internal flow of helium is 7.6 l/h and the flow of BFS is 8.9 ml/h. This is the same case as is illustrated in figure 4. In both cases, the bubble diameter is close to 0.65 mm with a quite narrow distribution. As expected, the time response for AFSB is positive. Compared to an earlier report on AFSB (Faleiros et al., 2018), the bubbles in the present study have almost twice the diameter, but a significantly smaller time response. This is surprising since equation (2) suggests that the time response should increase due to the larger diameter.

For the HFSB, the result of several combinations two different flow rates of BFS (8.9 ml/h and 11.0 ml/h) and a larger variation of the flow of helium is shown in figure 7. As noted by Faleiros et al. (2019), the bubble density can be calculated using conservation of mass and volume from the ratio between flow of helium, Q_{He} and the flow of BFS, Q_{BFS}. This requires mono-disperse bubbling and no "leakage" of helium and BFS. Leakage of helium could e.g. be caused by periods where the soap film in not enclosing the inner pipe exit inside the bubble generator. Leakage of BFS could e.g. be satellite drops formed during the bubble generation. Faleiros et al. (2019) experimentally found neutral bubbles for $Q_{He}/Q_{BFS} = 900$ while the theoretical value for perfect conservation is $Q_{He}/Q_{BFS} = 1080$. As seen in figure 7, the present experiments find a slightly negative time response for almost all values of Q_{He}/Q_{BFS} even though there is a weak trend for lower time response for larger values of Q_{He}/Q_{BFS}. This suggests some spillage of BFS, at least at apparent low values of Q_{He}/Q_{BFS}.

5 Discussion and conclusion

A new method to measure the time response of HFSB and AFSB has been developed and tested. The method appears to work and show that a new design for a bubble generator produces quite mono-disperse bubbles with a small time response and a narrow distribution of the time response. The mono-disperse property of the bubbles has been confirmed by shadow imaging of the bubble near the bubble generator. The tested AFSB appear to show that relatively large AFSB with a quite low time response, less than 100 μs, can be made. However, this should be investigated further since it contradicts earlier reports on AFSB.

Only relatively short data series have been taken for the present paper. The method should therefore be verified with a larger data material. It is somewhat surprising that a clearly positive time response is not observed for low values of Q_{He}/Q_{BFS}. The observations by Faleiros et al. (2019) also show considerable variation in the time response for different flow settings. The amount of data in the present paper is too low to draw a firm conclusion about time response variation from the tested bubble generator. Plots of the time history of observed time response (not shown) indicate regular small variation and small breaks in production. This could indicate that the bubble generator is not completely stable and that this phenomenon could be related to some spillage of BFS.

The test method can be developed into a compact transportable unit to be used to monitor bubble production at experiments. The camera could be replaced with a simpler and less expensive camera taking images with longer exposure time, if the light source is changed to give a train of short light pulses. This is relatively easy to build with a strong LED light source. Each bubble would then be recorded at several

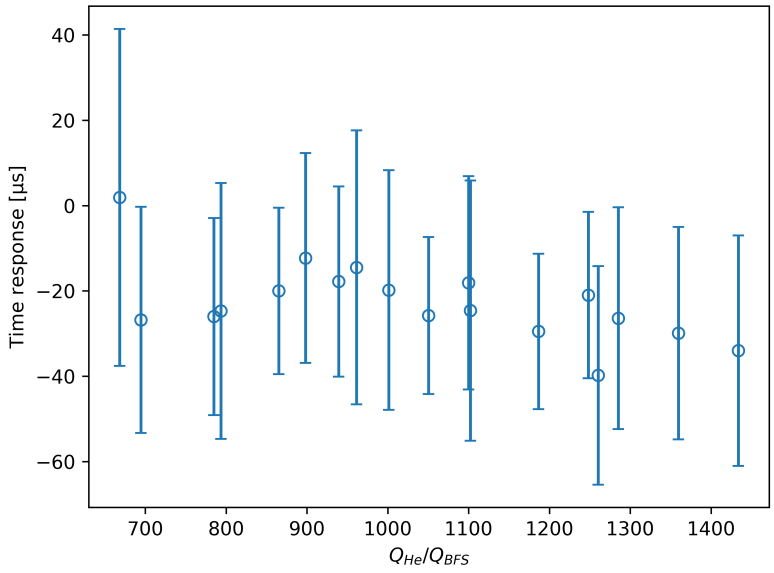

Figure 7: Time response as a function of the ratio between flow of helium and BFS. Errorbars indicate plus/minus one standard deviation of the observed variation in time response for each series.

positions along its path in a single frame. The current data processing can be used with only small changes.

References

Adrian RJ and Westerweel J (2011) *Particle Image Velocimetry*. Cambridge University Press

Bosbach J, Kühn M, and Wagner C (2009) Large scale particle image velocimetry with helium filled soap bubbles. *Experiments in Fluids* 46:539–547

Faleiros DE, Tuinstra M, Sciacchitano A, and Scarano F (2018) Helium-filled soap bubbles tracing fidelity in wall-bounded turbulence. *Experiments in Fluids* 59:56

Faleiros DE, Tuinstra M, Sciacchitano A, and Scarano F (2019) Generation and control of helium-filled soap bubbles for piv. *Experiments in Fluids* 60:40

Gibeau B and Ghaemi S (2018) A modular, 3d-printed helium-filled soap bubble generator for largescale volumetric flow measurements. *Experiments in Fluids* 59:178

Huhn F, Schanz D, Gesemann S, Dierksheide U, van de Meerendonk R, and Schröder A (2017) Large-scale volumetric flow measurement in a pure thermal plume by dense tracking of heliumfilled soap bubbles. *Experiments in Fluids* 58:116

Jux C, Sciacchitano A, Schneiders JFG, and Scarano F (2018) Robotic volumetric piv of a full-scale cyclist. *Experiments in Fluids* 59:74

Scarano F, Ghaemi S, Caridi GCA, Bosbach J, Dierksheide U, and Sciacchitano A (2015) On the use of heliumfilled soap bubbles for large-scale tomographic piv in wind tunnel experiments. *Experiments in Fluids* 56:42

White FM (2016) *Fluid Mechanics*. McGraw-Hill. 6 edition